

Inducible and neuronal nitric oxide synthases exert contrasting effects during rat intestinal recovery following fasting

Junta Ito, Hiroyuki Uchida, Naomi Machida, Kazuo Ohtake, Yuki Saito and Jun Kobayashi

Division of Pathophysiology, Faculty of Pharmaceutical Science, Department of Clinical Dietetics and Human Nutrition, Josai University, Saitama 350-0295, Japan

Corresponding author: Hiroyuki Uchida. Email: mrhiro@josai.ac.jp

Impact statement

Besides providing new data confirming the involvement of iNOS and nNOS in intestinal mucosal atrophy caused by fasting, this study details their expression and function during recovery from this condition following refeeding. We demonstrate a significant negative correlation between iNOS and nNOS levels during refeeding, and associate this with cell proliferation and apoptosis in crypts and villi. These novel findings elucidate the relationship between these NOS isoforms and its impact on recovery from intestinal injury. A mechanism is proposed comprising the up-regulation of nNOS activity by mechanical stimulation due to the presence of food in the intestine, restricting iNOS-associated apoptosis and promoting cell proliferation and gut motility. Our investigation sheds light on the molecular basis behind the repercussions of total parenteral nutrition on intestinal mucosal integrity, and more importantly, the beneficial effects of early enteral feeding.

Abstract

We investigated the effects of endogenous inducible (iNOS) and neuronal nitric oxide synthase on recovery from intestinal mucosal atrophy caused by fasting-induced apoptosis and decreased cell proliferation during refeeding in rats. Rats were divided into five groups, one of which was fed *ad libitum*, and four of which underwent 72 h of fasting, followed by refeeding for 0, 6, 24, and 48 h, respectively. iNOS and neuronal nitric oxide synthase mRNA and protein levels in jejunal tissues were measured, and mucosal height was histologically evaluated. Apoptotic indices, interferon- γ (IFN- γ) transcription levels, nitrite levels (as a measure of nitric oxide [NO] production), 8-hydroxydeoxyguanosine formation (indicating reactive oxygen species [ROS] levels), crypt cell proliferation, and the motility indices (MI) were also estimated. Associations between mucosal height and NOS protein levels were determined using Spearman's rank correlation test. Notably, we observed significant increases in mucosal height and in neuronal nitric oxide synthase mRNA and protein expression as refeeding time increased. Indeed, there was a significant positive correlation between neuronal nitric oxide synthase protein level and mucosal height during the 48-h refeeding period ($r = 0.725$, $P < 0.01$). Conversely, iNOS mRNA and protein expression decreased according to refeeding time, with a significant negative correlation between iNOS protein level and mucosal height being recorded during the 48-h refeeding period

($r = -0.898$, $P < 0.01$). We also noted a significant negative correlation between jejunal neuronal nitric oxide synthase and iNOS protein concentrations over this same period ($r = -0.734$, $P < 0.01$). Refeeding also restored the decreased jejunal MI caused by fasting. Our finding suggests that refeeding likely repairs fasting-induced jejunal atrophy by suppressing iNOS expression and subsequently inhibiting NO, ROS, and IFN- γ as apoptosis mediators, and by promoting neuronal nitric oxide synthase production and inducing crypt cell proliferation via mechanical stimulation.

Keywords: Intestinal atrophy, neuronal nitric oxide synthase, inducible nitric oxide synthase, refeeding, apoptosis

Experimental Biology and Medicine 2017; 242: 762–772. DOI: 10.1177/1535370217694434

Introduction

Prolonged fasting impairs intestinal physiology and causes intestinal barrier dysfunction, including increased epithelial permeability and compromised tight junctions, leading to bacterial translocation, particularly in patients receiving a prolonged course of total parenteral nutrition (TPN).^{1,2} Many surgeons involved in nutrition support therapy often observe the beneficial effects of early enteral feeding as opposed to protracted TPN, particularly regarding intestinal barrier functions and subsequent septic complications.^{3–5}

Early enteral feeding, therefore, represents a potentially important therapeutic intervention for the maintenance of intestinal mucosal homeostasis and integrity.

Under pathological conditions such as intestinal starvation during TPN, increased apoptosis and decreased cell proliferation are observed in the intestinal epithelium.^{6–8} Using histomorphometric analysis, we previously demonstrated comparable pathological changes in rats fasted for 72 h, comprising heightened apoptosis and reduced cell proliferation, predominantly in villi and crypts,⁹ suggesting the

involvement of a similar mechanism effecting such changes. In addition, this previous work attributed fasting-induced rat intestinal atrophy to jejunal inducible nitric oxide (NO) synthase (iNOS)-mediated apoptosis. Decreased neuronal NOS (nNOS) expression was also evident in rat intestine during fasting, suggesting roles for both nNOS and iNOS in the regulation of fasting-induced mucosal atrophy.

NO is a weak radical generated from L-arginine by the three NOS isoforms nNOS, iNOS, and endothelial NOS. NO is important in protection against bowel injury^{10,11} and iNOS plays a key role in this pathology. For instance, rat small intestines with histological abnormalities demonstrate increased iNOS expression.^{9,12} nNOS is the predominant isoform in the intestine, and its activity is inversely correlated with the extent of tissue injury.¹³

Previous investigations using animal models have suggested that nNOS and iNOS are key in the development and progression of post-inflammatory functional gastrointestinal disorders,¹⁴ ischemia-reperfusion injury (IRI), acute rejection (AR) in intestinal transplantation,¹⁵ and necrotizing enterocolitis (NEC).¹² The pathologies described in each of these studies involved increased iNOS and decreased nNOS levels.

However, the effect of iNOS and nNOS on recovery by refeeding from fasting-induced mucosal atrophy remains unclear. Therefore, a fundamental understanding of the underlying mechanisms operating during these processes is needed. The objective of the present study was to investigate the manner in which iNOS and nNOS affect rat intestinal healing associated with refeeding after mucosal atrophy caused by fasting-induced apoptosis and suppressed cell proliferation.

Materials and methods

Animals and experimental design

The current experimental protocol and design were approved by the Institutional Animal Care and Use Committee of the Life Science Center of Josai University. Nine-week-old male Wistar rats were purchased from SLC (Shizuoka, Japan) and housed individually in wire-bottom cages in a room illuminated from 7 a.m. to 7 p.m. (12:12-h light:dark cycle). Animals were allowed free access to deionized water and standard rat chow (CE-2; CLEA, Tokyo, Japan) until the study began. At 10 weeks of age, 35 rats were randomly divided into five groups. Four groups were fasted for 72 h, and refed for 0 (i.e. 72-h fasted), 6, 24, or 48 h. The remaining group was given *ad libitum* access to food as a normally fed control. Rats were weighed daily. Furthermore, jejunal peristalsis was measured in three rats to calculate the motility index (MI).

Collection of intestinal mucosa

After refeeding, rats were anesthetized and euthanized by exsanguination. The entire small intestine was carefully removed and placed on ice. Ten centimeters was removed from the oral (duodenum) side, and the remainder of the

intestine was divided into two segments: proximal (jejunum) and distal (ileum). Jejunum segments 3–5 cm distal to the duodenum were used in analyses.¹⁶ Samples approximately 3 cm in length were fixed in 10% neutral buffered formalin for measurement of mucosal height and immunohistochemistry. The remaining segments were snap-frozen in liquid nitrogen and stored at -80°C .

Histopathological analysis of mucosal height, apoptotic index, and cell proliferation

Tissue samples fixed in 10% neutral buffered formalin were embedded in paraffin and sectioned, before being stained with hematoxylin and eosin (H&E). Mucosal height (villous height plus crypt depth) was measured using a microscope (BX41; Olympus, Tokyo, Japan) and a digital camera system (Penguin 150CL; Pixera, San Jose, CA, USA). Mucosal height was measured for at least 30 villi per animal.

To measure enterocyte apoptosis in the jejunum, the apoptotic index (AI) was calculated by conventional light microscopy of H&E-stained specimens, following the methods of Dahly et al. and Ito et al.^{6,9} Terminal deoxynucleotidyl transferase dUTP nick-end labelling (TUNEL) staining of apoptotic cells is easy to interpret for all images; however, because of its nonspecific staining, representative apoptotic changes were utilized for the analysis of AI. In brief, jejunal sections as used above for histopathological analysis were examined in a blinded manner for the typical attributes of apoptotic cells. Fifty villus-crypt columns were assessed per rat. For each column, the number and position of apoptotic cells and the total number of cells were recorded. To measure the effects of fasting and refeeding on apoptosis, the average number of apoptotic cells in villi and crypts and the AI were determined. To ascertain the principal sites of apoptosis along the villi and crypts, AI distribution profiles were generated based on group means, in which cell position was plotted against the AI for that position. AI, in this case, was defined as the total number of apoptotic cells at each position expressed as a percentage of the total number of cells counted at that position. Position 1 was set as the cell at the crypt-villus junction, and that at the base of the crypt column, for villus and crypt data, respectively.

To assess cell proliferation in the crypt, conventional light microscopy of specimens immunohistochemically stained for 5-bromo-2'-deoxyuridine (5-BrdU) was used to calculate the cell proliferation index.¹⁷ Rats were given intraperitoneal injections of 100 mg/kg 5-BrdU before euthanasia. After paraffin embedding and sectioning, tissue sections were dewaxed and immersed in 3% hydrogen peroxide-methanol solution before being washed with phosphate-buffered saline (PBS) and denatured in 2 N hydrochloric acid. Following further PBS washing, the specimens were immersed in 0.1 M boric acid buffer (pH 8.5), incubated with 20 $\mu\text{g}/\text{mL}$ proteinase K at 37°C and then the reaction was terminated with PBS containing bovine serum albumin. The sections were then incubated with mouse anti-5-BrdU monoclonal antibody (1:50; Chemicon International, Billerica, MA, USA), with the exception of control samples, for which the primary antibody was

omitted. A biotinylated goat anti-mouse IgG secondary antibody (1:200; Vector Laboratories, Burlingame, CA, USA) was subsequently applied. Sections were then treated with a VECTASTAIN Elite ABC Kit (Vector Laboratories), and staining was visualized by color development following addition of diaminobenzidine. Finally, the sections were counterstained with hematoxylin and examined under a light microscope with a digital camera system. The number of labelled cells in at least 10 well-orientated longitudinal crypts was determined for each rat. Results are expressed as the number of 5-BrdU-labelled cells per crypt.

Immunohistochemical assessment of iNOS and nNOS expression

Immunohistochemical staining was performed with a rabbit anti-iNOS polyclonal antibody and a mouse anti-nNOS monoclonal antibody.¹⁸ The specimens were dewaxed and treated for antigen retrieval by boiling in 10 mM citrate buffer (pH 6.0).¹⁹ After being washed with PBS, they were then exposed to 6% hydrogen peroxide, and nonspecific binding was blocked with 20% goat serum in PBS. Specimens were subsequently incubated with one of the primary antibodies (1:100; BD Transduction Laboratories, Lexington, KY, USA), except for control sections, for which no primary antibody was used. Biotinylated goat anti-rabbit or goat anti-mouse IgG secondary antibodies (1:200; Vector Laboratories) were then added. The sections were treated with a VECTASTAIN Elite ABC Kit, and antibody binding was detected by color development after addition of diaminobenzidine. Finally, sections were counterstained with hematoxylin, and examined under a light microscope with a digital camera system.

Five clearly dyed sections were chosen randomly for each rat, and five random fields for each section were assessed (at 40× magnification). The presence of iNOS and nNOS was semi-quantitatively measured based on average optical density using a digital camera and ImageJ software (National Institutes of Health, Bethesda, MD, USA; <http://imagej.nih.gov/ij/>).¹²

Jejunal nitrite concentrations

Nitrite concentrations in the jejunum were measured using a dedicated high-performance liquid chromatography (HPLC) system (ENO-20; EiCom, Kyoto, Japan). Frozen jejunal segments were deproteinized by homogenization with an equal volume of methanol and centrifugation at $12,000 \times g$ for 5 min at 4°C.²⁰ The samples were then applied to the HPLC system. Nitrite and nitrate were separated using a reverse-phase column (NO-PAK; EiCom), after which nitrate was reduced to nitrite in a reduction column packed with copperised cadmium (NO-RED; EiCom). These nitrites were then mixed with Griess reagent in a reaction coil, and the change in absorbance was monitored at 540 nm.

Analysis of iNOS, nNOS, and interferon (IFN)- γ mRNA expression by reverse transcription-polymerase chain reaction (RT-PCR)

Total RNA was purified using RNA isoreagent (TaKaRa Bio, Kusatsu, Japan) and subjected to RT-PCR using an RNA PCR Kit (AMV) Version 3.0 (TaKaRa Bio), as follows: 42°C for 30 min, 99°C for 5 min, and 5°C for 5 min for reverse transcription; then 30 cycles of 94°C for 30 s, 60°C for 30 s, and 72°C for 1 min for PCR. The following primer pairs (synthesized by TaKaRa Bio) were used: iNOS forward, 5'-CTCACTGTGGCTGTGGTCACCTA-3'; iNOS reverse, 5'-GGGTCTTCGGGCTTCAGGTTA-3' (product size: 101 bp, TaKaRa Bio ID: RA008296); nNOS forward, 5'-TCAAAGCCATCCAGCGCATA-3'; nNOS reverse, 5'-GCGGTTGGTCACTTCATACGTTTC-3' (146 bp, RA022317); IFN- γ forward, 5'-AGGCCATCAGCAACAACATAAGTG-3'; IFN- γ reverse, 5'-GACAGCTTTGTGCTGGATCTGTG-3' (140 bp, RA021293). The expression of target mRNAs was normalized to that of glyceraldehyde 3-phosphate dehydrogenase (GAPDH), which was measured using the following primers: GAPDH forward, 5'-GGCACAGTCAAGGCTGA GAATG-3'; GAPDH reverse, 5'-ATGGTGGTGAAGACGC CAGTA-3' (143 bp, RA015380). An aliquot of each PCR was electrophoresed on a 2% agarose gel in Tris-borate-EDTA buffer, and DNA bands were visualized using ethidium bromide staining. PCR product intensity was measured using the Gene Genius Bioimaging System (Syngene, Cambridge, UK).

DNA oxidation analysis

Oxidative stress in the jejunum was evaluated by quantifying 8-hydroxydeoxyguanosine (8-OHdG) present in DNA.²¹ This molecule results from DNA oxidation and is produced by enzymatic cleavage after 8-hydroxylation of a guanine base. It is thought to be a marker of oxidative DNA damage reflecting the DNA repair rate.²² Jejunal DNA was purified using a DNA Extractor TIS Kit (Wako, Osaka, Japan).²³ DNA samples were hydrolyzed to nucleosides by sequential incubation with 6 U nuclease P1 (Wako) and 2 U alkaline phosphatase (Wako). Hydrolysates were filtered through Vivaspin 500 centrifugal concentrators with a molecular weight cut-off of 10,000 (Sartorius Stedim Biotech, Gottingen, Germany), and levels of 8-OHdG in the filtered samples were determined with an enzyme-linked immunosorbent assay kit (ELISA; Japan Institute for the Control of Aging, Shizuoka, Japan).

Jejunal motility

Nine-week-old male Wistar rats were operated upon during pentobarbital anesthesia (35 mg/kg Somnopentyl, administered intraperitoneally). Through a midline skin incision, a miniature strain gauge force transducer (FT-04IS; Star Medical, Tokyo, Japan) developed for *in vivo* small intestine motility studies of small animals was sutured around the circumference of the serosal surface of the jejunum, 4–5 cm distal to the ligament of Treitz.²⁴ In addition, a telemeter (IMT-101T; Star Medical) was sutured in the abdominal cavity of the left lower abdomen

quadrant. After 10 days to recover from the operation, rats were used in the experiment. Each rat was placed in a plastic cage on a receiver (IMT-10RA; Star Medical), the signals from which were relayed to a computer through a PowerLab 4/25 data acquisition system (AD Instruments, Tokyo, Japan). Rats were fasted for three days after *ad libitum* access to standard rat chow, before being refed for three days. Fasting and refeeding started at 9 a.m.

The recording of jejunal contractions was adjusted using software (Chart 5; AD Instruments) to correct for movements unrelated to intestinal motility. The MI, calculated using these modified measurements, was defined as the area under the contraction curves in each 30-min recording, and is expressed as a proportion of the mean MI recorded during the 24-h *ad libitum* feeding period prior to fasting.

Statistical analysis

Statistical analyses were performed using SPSS Version 22 for Windows (IBM, Armonk, NY, USA). All values are expressed as means \pm SE. One-way analysis of variance followed by Tukey's test was used to determine statistical differences between treatment groups. *P* values < 0.05 were considered statistically significant. Associations between mucosal height and NOS protein levels were analyzed using the Spearman's rank correlation test.

Results

Evaluation of intestinal mucosal height and nNOS and iNOS protein expression in fasted and refed rats

Table 1 shows body weights, mucosal heights, and nNOS and iNOS protein expression of rats in each treatment group. Rats fasted for 72 h (0 h refeeding) lost approximately 25% ($P < 0.01$) of their body weight compared with control rats fed *ad libitum*. After refeeding, gradual increases in body weight were observed. Although rats fasted for 72 h exhibited a greater degree of jejunal mucosal atrophy than those fed *ad libitum*, significant recovery ($P < 0.01$) of mucosal height was observed after 24 and 48 h of refeeding, compared with 0 h.

Staining of nNOS protein was mainly seen in the myenteric plexus and nerve fibers of the jejunal muscle layer (Figure 1). As shown in Table 1, quantitative measurement

using average optical densities revealed that nNOS expression decreased after fasting (0 h refeeding), i.e. compared with the *ad libitum* control, and was significantly increased after 6, 24, and 48 h of refeeding in comparison with the 0 h group ($P < 0.01$). Moreover, a significant positive correlation between nNOS protein level and mucosal height was apparent during the 48-h refeeding period ($r = 0.725$, $P < 0.01$). In contrast, iNOS protein was localized almost exclusively in the mucosal epithelial monolayer (Figure 1), and its expression increased following fasting (0 h refeeding) and was markedly reduced at each refeeding time point ($P < 0.01$, Table 1). We identified a significant negative correlation between iNOS protein expression and mucosal height during the 48 h of refeeding ($r = -0.898$, $P < 0.01$). In addition, there was a significant negative correlation between jejunal levels of nNOS and iNOS proteins over this same period ($r = -0.734$, $P < 0.01$).

Intestinal nNOS and iNOS mRNA expression

The expression of nNOS mRNA in jejunal tissues gradually increased in a refeeding-time-dependent manner (Figure 2), being significantly higher at the 24- and 48-h time points ($P < 0.05$ and $P < 0.01$, respectively, vs. 0 h). However, iNOS mRNA expression showed the opposite trend, decreasing as refeeding time increased, with significantly reduced levels after 24 and 48 h of refeeding (both $P < 0.01$ vs. 0 h).

NO, reactive oxygen species, and IFN- γ as apoptosis mediators

Since we previously determined that fasting causes jejunal apoptosis via reactive oxygen species (ROS) production and subsequent induction of IFN- γ transcription following increased iNOS expression,⁹ in the present work, we measured levels of nitrite (indicating NO production), 8-OHdG (as a marker of ROS presence), and IFN- γ mRNA (a ROS-mediated iNOS inducer). Consistent with the above-mentioned changes in iNOS transcription and translation, fasting increased intestinal nitrite levels ($P < 0.01$, 0 h vs. *ad libitum*), which were significantly reduced after refeeding ($P < 0.01$, Figure 3). Furthermore, the elevated jejunal 8-OHdG levels observed after fasting were substantially

Table 1 Evaluation of intestinal mucosal atrophy and nNOS and iNOS protein expression in fasted and refed rats

	Ad libitum	Refed			
		0 h	6 h	24 h	48 h
Body weight (g)	239.4 \pm 3.3	178.1 \pm 2.4*	199.3 \pm 4.0**†	202.7 \pm 5.5*†	205.3 \pm 2.3*†
Jejunum					
Mucosal height (μ m)	606.5 \pm 8.5	437.9 \pm 5.9*	465.9 \pm 8.6*	471.2 \pm 7.9*†	554.4 \pm 5.7*†
iNOS protein (optical density)	0.128 \pm 0.008	0.673 \pm 0.023*	0.426 \pm 0.020**†	0.077 \pm 0.017†	0.042 \pm 0.003*†
nNOS protein (optical density)	0.078 \pm 0.003	0.053 \pm 0.002*	0.086 \pm 0.003†	0.092 \pm 0.003*†	0.095 \pm 0.002*†

Note: Mucosal height (villous height plus crypt depth) was measured by observing H&E-stained specimens. Protein levels were assessed based on average optical densities of immunohistochemically stained tissue sections. *Ad libitum*: control rats with free access to food; 0 h, 6 h, 24 h, and 48 h represent the length of time for which rats were refed after 72 h of fasting. Values are means \pm SE. Seven rats were included in each group.

* $P < 0.01$ vs. *ad libitum*.

† $P < 0.01$ vs. 0 h refed.

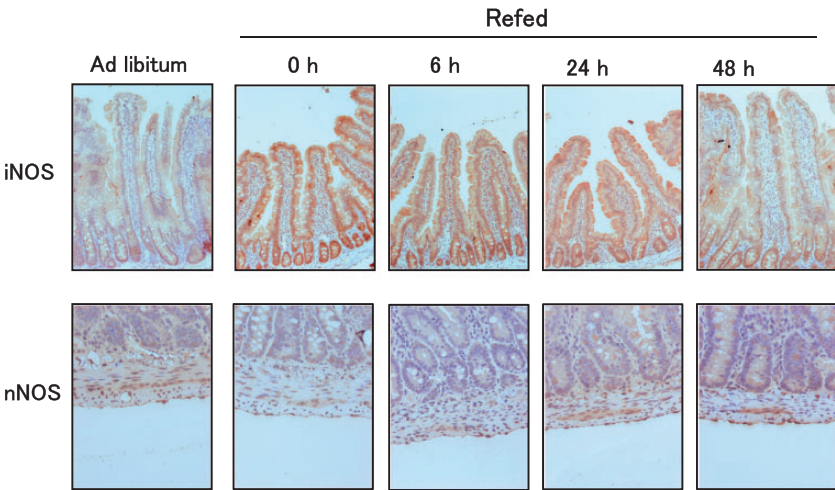


Figure 1 iNOS and nNOS protein expression in the jejunum of fasted and re-fed rats. Light micrographs of immunohistochemical staining for iNOS and nNOS. *Ad libitum*: control rats with free access to food; 0 h, 6 h, 24 h, and 48 h represent the length of time for which rats were re-fed after 72 h of fasting. Seven rats were included in each group. Magnification: 40 \times (iNOS); 100 \times (nNOS).

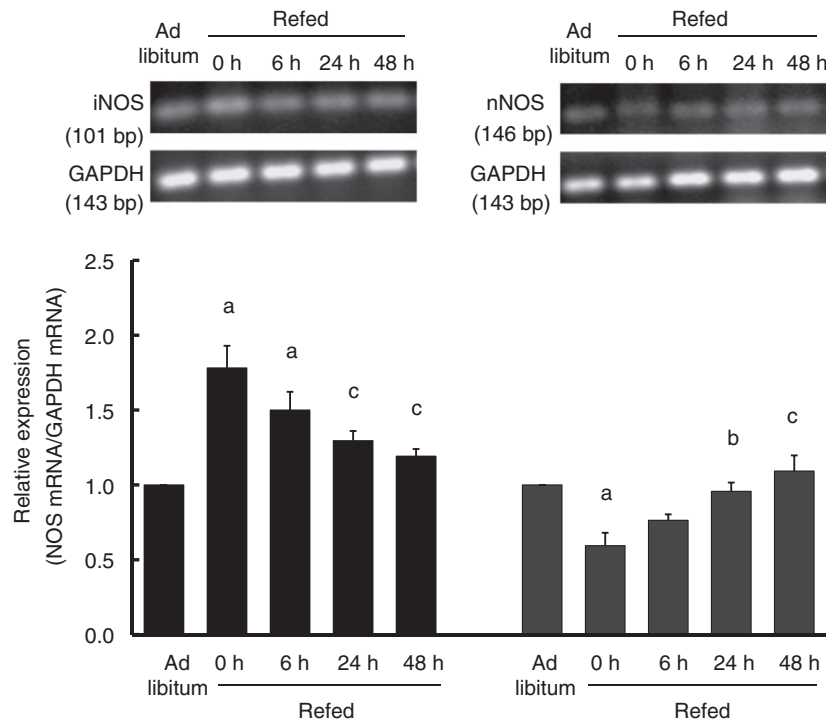


Figure 2 iNOS and nNOS mRNA expression in the jejunum of fasted and re-fed rats. RT-PCR products were visualized by electrophoresis (upper panels), and the intensities of the resulting bands were measured (lower charts). iNOS and nNOS expression levels were normalized to those of GAPDH. Values are means \pm SE. ^a $P < 0.01$ vs. *ad libitum*; ^b $P < 0.05$; ^c $P < 0.01$ vs. 0 h re-fed. Seven rats were included in each group.

diminished by 24 and 48 h of refeeding ($P < 0.05$ vs. 0 h, Figure 4). Transcription of IFN- γ , which increased as a result of fasting ($P < 0.01$), also significantly fell following refeeding ($P < 0.01$, Figure 5). These results mirrored the alterations observed in intestinal iNOS expression, suggesting that iNOS is regulated at the transcriptional level during fasting and refeeding through signalling mediators including ROS and IFN- γ .

Evaluation of enterocyte apoptosis in the jejunal mucosae of fasted and re-fed rats

Table 2 shows AIs for the villi and crypts of rats in each treatment group. Using histomorphometric assessment of jejunal cells, we evaluated the contribution of reduced apoptosis to recovery from fasting-induced mucosal atrophy following refeeding. The heightened villus AI recorded after 72 h of fasting (0 h refeeding) decreased at each

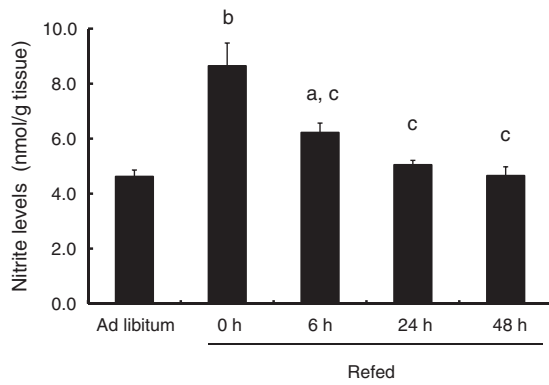


Figure 3 Nitrite levels in the jejunum of fasted and re-fed rats. HPLC was used to measure nitrite concentration as an indicator of NO production. Values are means \pm SE. ^a $P < 0.05$, ^b $P < 0.01$ vs. *ad libitum*; ^c $P < 0.01$ vs. 0 h re-fed. Seven rats were included in each group

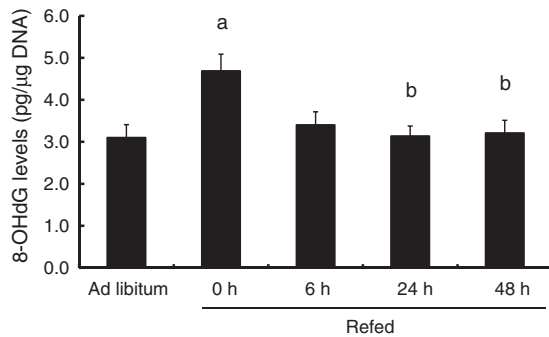


Figure 4 Levels of 8-OHdG in the jejunum of fasted and re-fed rats. ELISA was employed to assess the presence of 8-OHdG, a product of DNA oxidation and indicative of ROS production. Values are means \pm SE. ^a $P < 0.05$ vs. *ad libitum*; ^b $P < 0.05$ vs. 0 h re-fed. Seven rats were included in each group

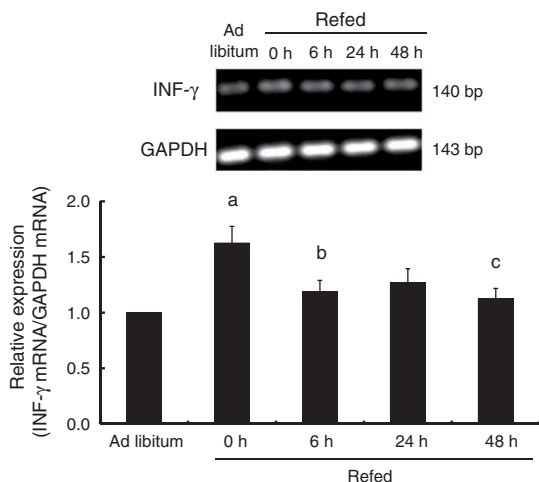


Figure 5 Expression of IFN- γ mRNA in the jejunum of fasted and re-fed rats. Data were collected and analyzed as in Figure 2. Values are means \pm SE. ^a $P < 0.01$ vs. *ad libitum*; ^b $P < 0.05$, ^c $P < 0.01$ vs. 0 h re-fed. Seven rats were included in each group

refeeding time point, with a significant difference ($P < 0.01$) in jejunal AI evident between the 0 and 48 h groups. AI distribution profiles (Figure 6(a)) determined by histomorphometry, which is preferable to TUNEL for quantitative assessment, showed increased apoptosis along the entire jejunal villus after fasting, with the lower half of this structure (cell positions 1–40) being predominantly affected at 0 h, before AIs at this location began to reduce due to refeeding. After 72 h of fasting, the AI observed in jejunal crypts was elevated, and significantly decreased at the 6- and 48-h refeeding time points ($P < 0.01$, Table 2). From the AI distribution profiles, increased apoptosis in the lower thirds of crypts (cell positions 1–10) was evident after fasting (Figure 6(b)), which diminished following refeeding. Notably, the increased apoptosis observed after fasting conspicuously decreased after 6-h refeeding, but slightly increased after 24- and 48-h refeeding, compared with the 6-h time point. These changes might be a cell response to the transition from fasting to feeding. This result was broadly consistent with changes in intestinal iNOS levels, indicating that enterocyte apoptosis may be regulated by iNOS expression during fasting and refeeding.

Evaluation of cell proliferation in the jejunal crypts of fasted and re-fed rats

To evaluate the importance of reduced cell proliferation in jejunal mucosal atrophy, we assessed 5-BrdU incorporation, a proliferation indicator, in the jejunum. Although cell proliferation decreased after 72 h of fasting (0 h refeeding) compared with the *ad libitum* feeding control, it rose significantly after 24 and 48 h of refeeding in comparison to the 0 h group ($P < 0.05$, Figure 7).

Jejunal MI

Figure 8 shows the effect of fasting and refeeding on jejunal motility. The MI decreased during the second and third days of fasting compared with the *ad libitum* feeding period, and was greatly depressed between approximately 4 a.m. and 12:00 noon in particular. By the second day of refeeding after fasting for three days, the MI was higher than during the fasting period, and from 4 a.m. to 12:00 noon, had increased to nearly the level observed with *ad libitum* feeding. Decreased jejunal motility caused by fasting was restored after refeeding, reflecting the pattern of nNOS expression in response to these same events. Thus, both crypt cell proliferation and the jejunal MI were consistent with intestinal expression of nNOS, the transcription of which may therefore be regulated according to the absence or presence of luminal mechanical stimuli affecting the jejunal mucosa during fasting and refeeding.

Discussion

We previously showed that fasting causes intestinal mucosal atrophy resulting from increased apoptosis in jejunal villi, ROS production, and IFN- γ transcription following elevated iNOS expression, and decreased cell proliferation in jejunal crypts.⁹ As these apoptosis mediators are all suppressed by treatment with the iNOS inhibitor

Table 2 Enterocyte apoptosis in the jejunal mucosae of fasted and refed rats

		Refed			
		0 h	6 h	24 h	48 h
Ad libitum					
Villus					
Cells per villus column, <i>n</i>	88 ± 2	65 ± 1*	70 ± 1*	70 ± 1*	77 ± 1*,†
Apoptotic cells per villus column, <i>n</i>	0.05 ± 0.01	0.32 ± 0.03*	0.29 ± 0.03*	0.25 ± 0.03*	0.13 ± 0.04†
Apoptotic index (%)	0.06 ± 0.01	0.49 ± 0.05*	0.42 ± 0.05*	0.35 ± 0.05*	0.17 ± 0.05†
Crypt					
Cells per crypt column, <i>n</i>	28 ± 0.1	22 ± 0.1*	22 ± 0.3*	23 ± 0.1*	25 ± 0.3*,†
Apoptotic cells per crypt column, <i>n</i>	0.07 ± 0.00	0.18 ± 0.02*	0.05 ± 0.01†	0.13 ± 0.02‡	0.10 ± 0.01†
Apoptotic index (%)	0.25 ± 0.01	0.81 ± 0.08*	0.25 ± 0.07†	0.56 ± 0.07*	0.41 ± 0.05†

Note: Apoptosis was measured as in Figure 6. Values are means ± SE. Seven rats were included in each group.

**P* < 0.01 vs. *ad libitum*.

†*P* < 0.01 vs. 0 h refed.

‡*P* < 0.05 vs. *ad libitum*.

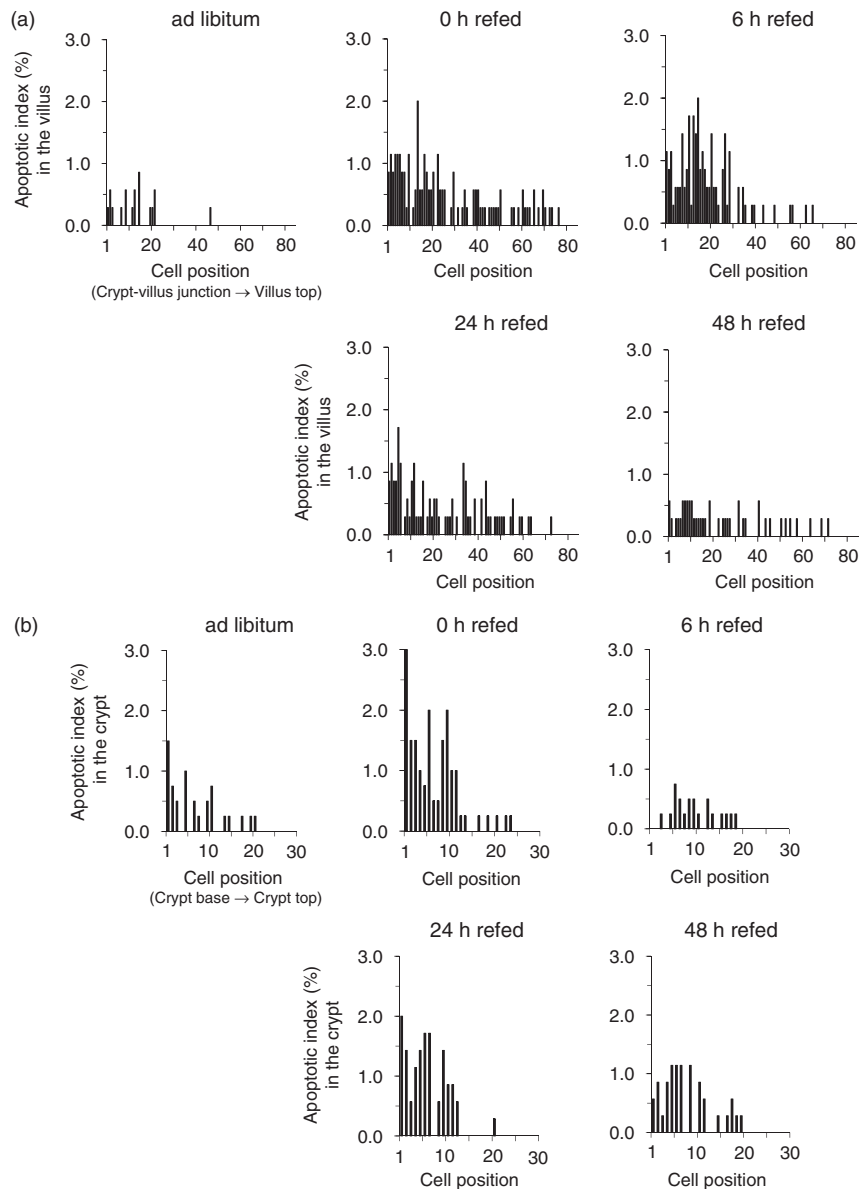


Figure 6 AI distribution profiles in the jejunal mucosae of fasted and refed rats. (a) AI distribution profiles in the villus. (b) AI distribution profiles in the crypt. AI was defined as the total number of apoptotic cells at each position expressed as a percentage of the total number of cells counted at that position. Position 1 was defined as the cell at the crypt-villus junction, and that at the base of the crypt for the villus and crypt data, respectively. Apoptosis was detected by histomorphometric assessment of H&E-stained tissue specimens. Seven rats were included in each group

aminoguanidine, with consequent mucosal recovery, iNOS is likely to be a significant upstream factor promoting fasting-induced apoptosis in intestinal epithelial cells. Furthermore, in contrast to the increase in iNOS transcription observed, we found that fasting decreased jejunal nNOS mRNA levels.

A small number of previous studies have also evaluated the roles of iNOS and nNOS in the intestine. For instance, Masaoka et al. investigated the occurrence of nitergic dysfunction and intestinal inflammation and dysmotility in normoglycaemic diabetes-prone animals,¹⁴ and Li et al. evaluated the role of these NOSs in IRI and AR following rat intestine transplantation, by administration of an NO inhibitor.¹⁵ In addition, Lu et al. assessed NOS functions and expression changes in neonatal rats subjected to lipopolysaccharide (LPS)-induced intestinal injury, describing an association between NEC and NOS levels in the mucosa.¹² The results of these studies suggest that increased iNOS and decreased nNOS mRNA and protein

levels contribute to each of the pathologies examined. Observations of the modulation of iNOS and nNOS expression are important when considering diseases of the small intestine or recovery from small intestinal injury.

The absence of food passing through the gastrointestinal tract during fasting represents a physiological challenge evoking functional and morphological changes in response to the lack of luminal nutrients^{1,25–27} and mechanical stimuli, including peristalsis and villous motility.^{28–30} The function and morphology of the small intestinal epithelium is precisely maintained by apoptosis and cell proliferation.^{31–33} Previous reports have demonstrated that fasting-induced apoptosis and suppressed cell proliferation are principally regulated by luminal nutrition or mechanical stimuli.^{1,27,29} Based on these findings, and because refeeding following fasting ameliorates jejunal mucosal atrophy,^{26,34} we supposed that refeeding might rescue the apoptosis and suppress cell proliferation resulting from lack of food, and that control of iNOS and nNOS expression may be associated with recovery from mucosal injury.

Recently, Qu and colleagues demonstrated that nNOS, the predominant NOS isoform (>90%) in the rat small intestine, suppresses constitutive expression of iNOS under normal conditions through nuclear factor-kappa B (NF- κ B) down-regulation. Moreover, nNOS inhibition leads to I κ B α degradation, followed by NF- κ B activation and a subsequent increase in iNOS expression.³⁵ Recent and accumulating evidence has revealed that under physiological conditions, NF- κ B proteins are inhibited by S-nitrosylation of critical cysteine residues, perhaps due to constitutive production of NO by NOS.³⁶ It is possible that intestinal nNOS suppression during fasting up-regulates NF- κ B, leading to iNOS induction. nNOS activation during refeeding may then inhibit NF- κ B, leading to iNOS suppression. Therefore, we hypothesized that iNOS activity is regulated by nNOS during recovery by refeeding

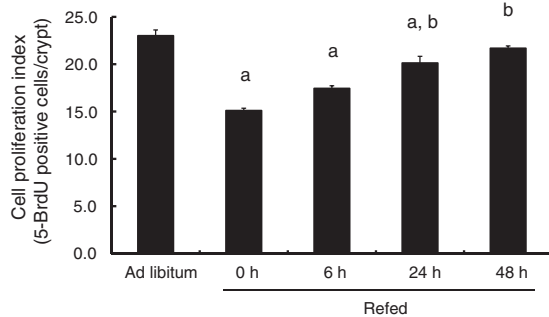


Figure 7. Cell proliferation indices of the jejunal crypts of fasted and refeed rats. Immunohistochemical staining was used to count the number of 5-BrdU-positive cells. Values are means \pm SE. ^a $P < 0.05$ vs. *ad libitum*; ^b $P < 0.05$ vs. 0 h refeed. Seven rats were included in each group

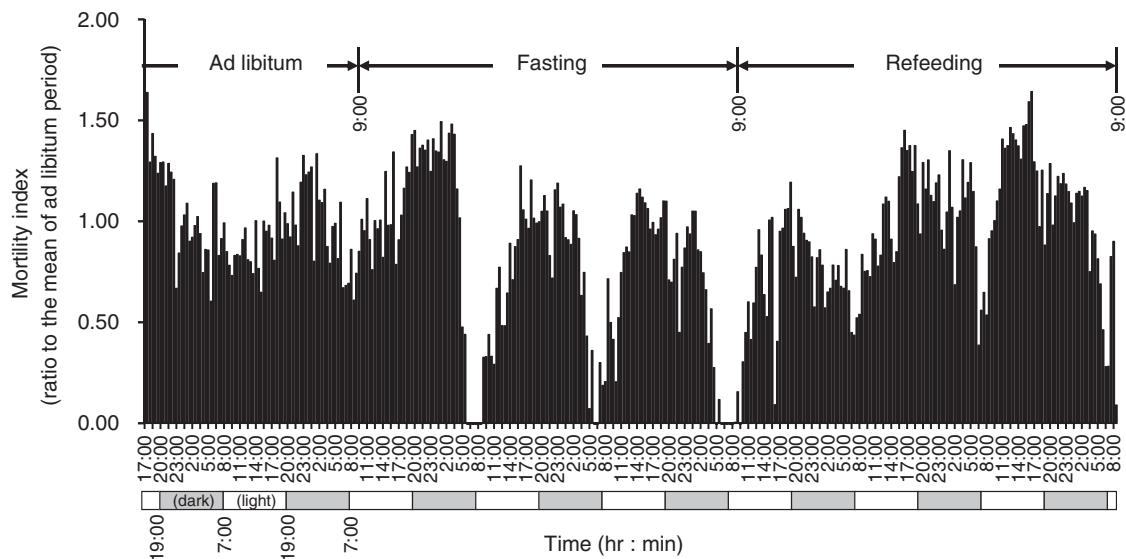


Figure 8 Jejunal MIs of fasted and refeed rats. A miniature strain gauge force transducer was surgically inserted into the abdomens of rats to record jejunal contractions. The MI is expressed as a proportion of the mean MI recorded during the 24-h *ad libitum* period. The results of one experiment, representative of the three experiments performed, are shown

from rat intestinal mucosal atrophy caused by fasting-induced apoptosis and suppressed cell proliferation.

There have been few reports regarding the involvement of iNOS in fasting-induced intestinal mucosal atrophy, and even fewer concerning nNOS. More importantly, the roles of these enzymes in recovery from this condition by refeeding have not yet been described. The objective of the present study was to examine the effects of refeeding on intestinal mucosal recovery from fasting-induced apoptosis and suppressed cell proliferation, with a particular focus on the possible participation of intestinal nNOS and iNOS in this process.

Here, we found that intestinal mucosal atrophy following fasting was remedied by refeeding, evident from increased mucosal height and accompanied by elevated nNOS and decreased iNOS protein levels, associated with reduced apoptosis (Table 1). iNOS and nNOS mRNA expression was consistent with this (Figure 2). We identified a negative correlation between iNOS and nNOS expression associated with recovery from mucosal atrophy. This is supported by the fact that nNOS is known to suppress iNOS transcription.³⁵

Although fasting caused increased production of NO, ROS, and IFN- γ as apoptosis mediators following elevation of iNOS expression,⁹ refeeding inhibited NO and ROS generation and IFN- γ induction, after decreasing iNOS levels (Figures 3 to 5). We used histomorphometric assessment of apoptotic changes in the jejunum to evaluate the importance of changes in apoptosis to intestinal recovery during refeeding. The raised AI recorded in villi and crypts after 72 h of fasting decreased with refeeding (Table 2). In addition, AI distribution profiles generated to identify the location of apoptotic enterocytes showed increased apoptosis along the length of jejunal villi after fasting, with the lower halves of such structures being particularly affected before recovery following refeeding (Figure 6(a)). The lower third of crypt cells also exhibited heightened apoptosis after removal of food, which diminished with refeeding (Figure 6(b)).

Boza et al. also tested the effect of refeeding on intestinal repair in fasted rats.²⁶ As in the present study, re-fed rats were found to have lower levels of apoptosis in the small intestine than fasted controls. Kakimoto et al. investigated intestinal mucosal apoptosis in rats fasted and subsequently fed expanded polystyrene as an indigestible material.²⁹ They observed a decrease in fasting-induced apoptosis due to the luminal mechanical stimulus provided by the presence of polystyrene in the intestine. Therefore, together with the present study, this suggests that luminal mechanical stimuli may mitigate increased intestinal apoptosis caused by fasting, and that intestinal iNOS activity might be regulated by nNOS in this process.

The results of the current investigation also indicated that suppression of cell proliferation during fasting was restored by refeeding (Figure 7). With TPN, as in fasting, the gastrointestinal tract goes unused, resulting in mucosal atrophy. Xiao et al. demonstrated that oral glutamate supplementation prevents intestinal atrophy in a mouse model of TPN.²⁷ TPN decreased proliferating cell nuclear antigen (PCNA) mRNA and protein expression, used as an

indicator of cell proliferation in mucosal crypts, whereas oral administration of glutamate, making it the sole luminal nutrient, prevented PCNA down-regulation during TPN. However, cell proliferation in intestinal crypts appears to be controlled by not only luminal nutrients, but also mechanical stimuli. Chaturvedi et al. investigated whether Src and Rac1 mediate deformation-induced FAK and ERK phosphorylation and proliferation of intestinal epithelial cells.²⁸ Repetitive deformation due to peristalsis and villous motility was found to promote such proliferation *in vitro* via a pathway involving these four molecules. Spencer et al. demonstrated that longitudinal mechanical stretching induces small intestinal growth *in vivo*, while maintaining its function.³⁰ The stretched bowel demonstrated a marked increase in crypt depth, accompanied by dramatically enhanced epithelial proliferation. Similar luminal mechanical stimuli resulting from refeeding induced proliferation of the intestinal epithelium, resulting in repair of mucosal atrophy.

In the present work, we demonstrated that decreased jejunal motility following fasting was restored by refeeding (Figure 8). These changes were accompanied by a corresponding reduction and increase in nNOS expression during fasting and refeeding, respectively (Table 1, Figure 2). A number of articles have addressed nNOS expression in relation to intestinal motility. Sasselli et al. investigated the ability of embryonic stem (ES) cells to respond to environmental cues relayed by the enteric nervous system (ENS) and associated tissues.³⁷ Expression of nNOS, regarded as a key molecule in the regulation of gastrointestinal motility, was observed to be induced in ES cells co-cultured with gut tissue comprising longitudinal muscle and adherent myenteric plexus. Furthermore, Grasa et al. established that down-regulation of nNOS is associated with rabbit intestinal dysmotility caused by local administration of LPS.³⁸ Several reports have noted a decrease in nNOS expression in the absence of mechanical stimuli in the small intestinal lumen during fasting.^{9,39} The current work provides further support for the relationship between mechanical stimuli and nNOS. Nakao et al. investigated whether nNOS expression in the myenteric plexus is regulated by the vagus or splanchnic nerves of the rat small intestine,⁴⁰ finding it to be independent of the former, but negatively regulated by the latter. The presence of an alimentary bolus in the gastrointestinal tract attenuates stimulation of the splanchnic nerves, and as a result, nNOS expression increases and jejunal motility may be promoted. We suggest that luminal mechanical stimulation caused by refeeding induces nNOS expression and subsequent jejunal motility.

If this is the case, additional questions are raised regarding the mechanism by which changes in intestinal motility provoked by fasting or refeeding, in other words the absence or presence of luminal mechanical stimuli, affect nNOS activity. This remains unclear because very few studies concerning these issues have been carried out. Under normal conditions, enterocyte apoptosis is confined to villi apices,⁴¹ whereas apoptotic cells in fasting rats are distributed throughout the whole intestine, being predominantly localized in the mucosa in close proximity to crypts and the myenteric plexus, where nNOS-containing neurons are

abundant.^{42,43} In the present study, histomorphometric assessment suggested that the reduction in apoptosis observed during refeeding principally took place in the lower halves of villi and lower thirds of crypts, while cell proliferation appeared to increase in the crypts, where nNOS activity may be restored by refeeding (Figure 6(a) and (b) and Figure 7). nNOS-positive neurons in the myenteric plexus receive sensory inputs from mucosal signals relayed by intrinsic primary afferent neurons (IPANs). IPANs are activated by the contents of the intestine, initiating peristalsis⁴⁴ and transmitting NO and acetylcholine signals from the myenteric plexus to mainly circular muscles through inhibitory and excitatory motor pathways projecting anally and orally, respectively.⁴⁵ Although nNOS-positive motor neurons are yet to be identified in the mucosa and submucosa, the terminals of nerves originating in the myenteric plexus have been observed scattered in these intestinal layers.⁴⁶ Some of these nerves are linked to the submucosal plexus, involved in secretomotor and vasomotor reflexes through vasoactive intestinal polypeptide (VIP) and VIP-mediated NO signalling,^{47–49} suggesting that mucosal secretion and vasodilation following feeding might be at least partially controlled by nitrergic neurons of the ENS.

As these reflexes are activated by mechanical stimuli acting on the bowel mucosa during feeding, intestinal motility provoked by fasting or refeeding might affect nNOS activity. This is supported by the findings of the present study, which implied that luminal mechanical stimulation caused by refeeding after fasting induced nNOS expression and subsequently, jejunal motility.

In conclusion, the present study showed that refeeding rescues intestinal nNOS activity by luminal mechanical stimulation of the lumen, and potentially restores mucosal homeostasis by suppressing iNOS-induced apoptosis and increasing nNOS-induced cell proliferation.

Authors' contribution: JI and HU contributed equally to this work. JI, HU, KO, and JK designed the study; JI, HU, NM, KO, and YS conducted the experiments and analyzed the data; JI and HU wrote the paper; HU and JK critically revised and reviewed the manuscript for important intellectual content.

ACKNOWLEDGEMENTS

We would like to thank Editage (www.editage.jp) for English language editing. This work was supported by the Ministry of Education, Culture, Sports, Science and Technology of Japan under Scientific Research (C) Grant-In-Aid 22591492 (to H. Uchida).

DECLARATION OF CONFLICTING INTERESTS

The author(s) declared no potential conflicts of interest with respect to the research, authorship, and/or publication of this article.

REFERENCES

- Shaw D, Gohil K, Basson MD. Intestinal mucosal atrophy and adaptation. *World J Gastroenterol* 2012;**18**:6357–75
- Buchman AL, Moukarzel AA, Bhuta S, Belle M, Ament ME, Eckhart CD, Hollander D, Gornbeln J, Kopple JD, Vijayaraghavan SR. Parenteral nutrition is associated with intestinal morphologic and functional changes in humans. *JPEN* 1995;**19**:453–60
- Peter JV, Moran JL, Phillips-Hughes J. A metaanalysis of treatment outcomes of early enteral versus early parenteral nutrition in hospitalized patients. *Crit Care Med* 2005;**33**:213–20
- Thomson A. The enteral vs parenteral nutrition debate revisited. *JPEN* 2008;**32**:474–81
- McClave SA, Martindale RG, Vanek VW, McCarthy M, Roberts P, Taylor B, Ochoa JB, Napolitano L, Cresci G the A.S.P.E.N. Board of Directors, the American College of Critical Care Medicine. Guidelines for the Provision and Assessment of Nutrition Support Therapy in the Adult Critically Ill Patient: Society of Critical Care Medicine (SCCM) and American Society for Parenteral and Enteral Nutrition (A.S.P.E.N.). *JPEN* 2009;**33**:277–316
- Dahly EM, Guo Z, Ney DM. Alterations in enterocyte proliferation and apoptosis accompany TPN-induced mucosal hypoplasia and IGF-I-induced hyperplasia in Rats. *J Nutr* 2002;**132**:2010–4
- Feng Y, Teitelbaum DH. Epidermal growth factor/TNF- α transactivation modulates epithelial cell proliferation and apoptosis in a mouse model of parenteral nutrition. *Am J Physiol Gastrointest Liver Physiol* 2012;**302**:G236–49
- Brinkman AS, Murali SG, Hitt S, Solverson PM, Holst JJ, Ney DM. Enteral nutrients potentiate glucagon-like peptide-2 action and reduce dependence on parenteral nutrition in a rat model of human intestinal failure. *Am J Physiol Gastrointest Liver Physiol* 2012;**303**:G610–22
- Ito J, Uchida H, Yokote T, Ohtake K, Kobayashi J. Fasting-induced intestinal apoptosis is mediated by inducible nitric oxide synthase and interferon- γ in rat. *Am J Physiol Gastrointest Liver Physiol* 2010;**298**:G916–26
- Kubes P, McCafferty DM. Nitric oxide and intestinal inflammation. *Am J Med* 2000;**109**:150–8
- Chokshi NK, Guner YS, Hunter CJ, Upperman JS, Grishin A, Ford HR. The role of nitric oxide in intestinal epithelial injury and restitution in neonatal necrotizing enterocolitis. *Semin Perinatol* 2008;**32**:92–9
- Lu H, Zhu B, Xue XD. Role of neuronal nitric oxide synthase and inducible nitric oxide synthase in intestinal injury in neonatal rats. *World J Gastroenterol* 2006;**12**:4364–8
- Qu XW, Wanga H, Rozenfeldb RA, Huang W, Hsueh W. Type I nitric oxide synthase (NOS) is the predominant NOS in rat small intestine. Regulation by platelet-activating factor. *Biochimica et Biophysica Acta* 1999;**1451**:211–7
- Masaoka T, Vanuytsel T, Vanormelingen C, Kindt S, Rasool SS, Boesmans W, Hertogh GD, Farré R, Berghe PV, Tack J. A spontaneous animal model of intestinal dysmotility evoked by inflammatory nitrergic dysfunction. *PLoS One* 2014;**9**:e95879
- Li XL, Zou XM, Nie G, Song ML, Li G. Roles of neuronal nitric oxide synthase and inducible nitric oxide synthase in intestinal transplantation of rats. *Transplant Proc* 2013;**45**:2497–501
- Fujise T, Iwakiri R, Wu B, Amemori S, Kakimoto T, Yokoyama F, Sakata Y, Tsunada S, Fujimoto K. Apoptotic pathway in the rat small intestinal mucosa is different between fasting and ischemia-reperfusion. *Am J Physiol Gastrointest Liver Physiol* 2006;**291**:G110–6
- Tang Y, Swartz-Basile DA, Swietlicki EA, Yi L, Rubin DC, Levin MS. Bax is required for resection-induced changes in apoptosis, proliferation, and members of the extrinsic cell death pathways. *Gastroenterology* 2004;**126**:220–30
- Morin MJ, Karr SM, Faris RA, Gruppuso PA. Developmental variability in expression and regulation of inducible nitric oxide synthase in rat intestine. *Am J Physiol Gastrointest Liver Physiol* 2001;**281**:G552–9
- Shi SR, Chaiwun B, Young L, Cote RJ, Taylor CR. Antigen retrieval technique utilizing citrate buffer or urea solution for

- immunohistochemical demonstration of androgen receptor in formalin-fixed paraffin sections. *J Histochem Cytochem* 1993;**41**:1599–604
20. Ohtake K, Ishiyama Y, Uchida H, Muraki E, Kobayashi J. Dietary nitrite inhibits early glomerular injury in streptozotocin-induced diabetic nephropathy in rats. *Nitric Oxide* 2007;**17**:75–81
 21. Inoue S, Kawanishi S. Oxidative DNA damage induced by simultaneous generation of nitric oxide and superoxide. *FEBS Lett* 1995;**371**:86–8
 22. Shigenaga MK, Gimeno CJ, Ames BN. Urinary 8-hydroxy-2'-deoxyguanosine as a biological marker of in vivo oxidative DNA damage. *Proc Natl Acad Sci USA* 1989;**86**:9697–701
 23. Saito S, Yamaguchi H, Hasui Y, Kurashige J, Ochi H, Yoshida K. Quantitative determination of urinary 8-hydroxydeoxyguanosine (8-OHdG) by using ELISA. *Res Commun Mol Pathol Pharmacol* 2000;**107**:39–44
 24. Watanabe T, Tomomasa T, Kaneko H, Takahashi A, Tabata M, Hussain S, Morikawa A. Involvement of serotonin and nitric oxide in endotoxin-induced gastric motility changes in conscious rats. *Dig Dis Sci* 2002;**47**:1284–9
 25. Carey HV, Hayden UL, Tucker KE. Fasting alters basal and stimulated ion transport in piglet jejunum. *Am J Physiol* 1994;**267**:R156–63
 26. Boza JJ, Möennoz D, Vuichoud J, Jarret AR, Gaudard-de-Weck D, Fritsché R, Donnet A, Schiffrin EJ, Perruisseau G, Ballèvre O. Food deprivation and refeeding influence growth, nutrient retention and functional recovery of rats. *J Nutr* 1999;**129**:1340–6
 27. Xiao W, Feng Y, Holst JJ, Hartmann B, Yang H, Teitelbaum DH. Glutamate prevents intestinal atrophy via luminal nutrient sensing in a mouse model of total parenteral nutrition. *FASEB J* 2014;**28**:2073–87
 28. Chaturvedi LS, Marsh HM, Shang X, Zheng Y, Basson MD. Repetitive deformation activates focal adhesion kinase and ERK mitogenic signals in human Caco-2 intestinal epithelial cells through Src and Rac1. *J Biol Chem* 2007;**282**:14–28
 29. Kakimoto T, Fujise T, Shiraishi R, Kuroki T, Park JM, Ootani A, Sakata Y, Tsunada S, Iwakiri R, Fujimoto K. Indigestible material attenuated changes in apoptosis in the fasted rat jejunal mucosa. *Exp Biol Med* 2008;**233**:310–6
 30. Spencer AU, Sun X, El-Sawaf MI, Haxhija EQ, Yang H, Brei DE, Luntz JE, Teitelbaum DH. Enterogenesis using an implantable mechanotransduction device. *J Surg Res* 2006;**130**:189–90
 31. Rao JN, Wang JY. *Regulation of gastrointestinal mucosal growth*. San Rafael, CA: Morgan & Claypool Life Sciences, 2010
 32. Aw TY. Cellular redox: a modulator of intestinal epithelial cell proliferation. *News Physiol Sci* 2003;**18**:201–4
 33. Fujimoto K, Iwakiri R, Wu B, Fujise T, Tsunada S, Ootani A. Homeostasis in the small intestinal mucosa balanced between cell proliferation and apoptosis is regulated partly by the central nervous system. *J Gastroenterol* 2002;**37**:139–44
 34. Dunel-Erb S, Chevalier C, Laurent P, Bach A, Decrock F, Maho YL. Restoration of the jejunal mucosa in rats refed after prolonged fasting. *Comp Biochem Physiol A Mol Integr Physiol* 2001;**129**:933–47
 35. Qu XW, Wang H, De Plaen IG, Rozenfeld RA, Hsueh W. Neuronal nitric oxide synthase (NOS) regulates the expression of inducible NOS in rat small intestine via modulation of nuclear factor kappa B. *FASEB J* 2001;**15**:439–46
 36. Hess DT, Matsumoto A, Kim SO, Marshall HE, Stamler J. Protein S-nitrosylation: purview and parameters. *Nat Rev Mol Cell Biol* 2005;**6**:150–66
 37. Sasselli V, Micci MA, Kahrig KM, Pasricha PJ. Evaluation of ES-derived neural progenitors as a potential source for cell replacement therapy in the gut. *BMC Gastroenterol* 2012;**12**:81
 38. Grasa L, Arruebo MP, Plaza MA, Murillo MD. A downregulation of nNOS is associated to dysmotility evoked by lipopolysaccharide in rabbit duodenum. *J Physiol Pharmacol* 2008;**59**:511–24
 39. Grongnet JF, David JC. Reciprocal variations of nNOS and HSP90 are associated with fasting in gastrointestinal tract of the piglet. *Dig Dis Sci* 2003;**48**:365–72
 40. Nakao K, Takahashi T, Utsunomiya J, Owyang C. Extrinsic neural control of nitric oxide synthase expression in the myenteric plexus of rat jejunum. *J Physiol* 1998;**507**:549–60
 41. Ramachandran A, Madesh M, Balasubramanian KA. Apoptosis in the intestinal epithelium: its relevance in normal and pathophysiological conditions. *J Gastroen Hepatol* 2000;**15**:109–20
 42. Ekblad E, Alm P, Sundler F. NOS-containing neurons in the gut and coeliac ganglia. *Neuropharmacology* 1994;**33**:1323–31
 43. Ekblad E, Mulder H, Uddman R, Sundler F. Distribution, origin and projections of nitric oxide synthase-containing neurons in gut and pancreas. *Neuroscience* 1994;**63**:233–48
 44. Kunze WAA, Furness JB. The enteric nervous system and regulation of intestinal motility. *Annu Rev Physiol* 1999;**61**:117–42
 45. Olsson C, Holmgren S. The control of gut motility. *Comp Biochem Phys A* 2001;**128**:481–503
 46. Costa M, Brookes SJH, Hennig GW. Anatomy and physiology of the enteric nervous system. *Gut* 2000;**47**:15–9
 47. Chino Y, Fujimura M, Kitahama K, Fujimiya M. Colocalization of NO and VIP in neurons of the submucous plexus in the rat intestine. *Peptides* 2002;**23**:2245–50
 48. Furness JB, Jones C, Nurgali K, Clerc N. Intrinsic primary afferent neurons and nerve circuits within the intestine. *Prog Neurobiol* 2004;**72**:143–64
 49. Toda N, Herman A. Gastrointestinal function regulation by nitrergic efferent nerves. *Pharmacol Rev* 2005;**57**:315–38

(Received October 15, 2016, Accepted January 26, 2017)